JOURNAL OF SPACECRAFT AND ROCKETS
Vol. 48, No. 1, January–February 2011

New Star-Pattern Identification Using a Correlation Approach for Spacecraft Attitude Determination

Hyosang Yoon*
Satrec Initiative, Daejeon 305-811, Republic of Korea
and
Yeerang Lim† and Hyochoong Bang‡
Korea Advanced Institute of Science and Technology, Daejeon 305-701, Republic of Korea

DOI: 10.2514/1.49675

A new star-pattern identification algorithm using correlation pattern-matching is proposed in this study. The new approach is based upon maximizing the target cost function, which is formed by the correlation between an original image and a target image. The image is reconstructed from the centroid positions of stars that are modeled as two-dimensional Gaussian functions. The correlation function in the form of cross-convolution in the image plane can be expressed by Fourier transform, so it is constructed analytically using only the centroid positions of stars in the image plane. The proposed algorithm compared with conventional pattern-matching techniques is simpler and more reliable, as verified by simulation study.

Nomenclature

$A(x, y)$	=	original star-pattern image
$A(\omega)$, $B(\omega)$	=	Fourier transform of one-dimensional signal
$a(x)$, $b(x)$	=	one-dimensional signal
$B(x, y)$	=	similar image in star catalog
$H(x)$	=	cross-correlation in frequency domain
$h(x)$	=	cross-correlation in spatial domain
J	=	cost function for two-dimensional images
J_0	=	cost function for one-dimensional signals
x_n	=	centroid position in x axis of n-th star
y_n	=	centroid position in y axis of n-th star
σ^2	=	variance of normal distribution
$\overline{(\cdots)}$	=	complex conjugate of $(\cdots)$

I. Introduction

ATTITUDE determination of spacecraft is a critical element for any space mission, from those centering on Earth observation to voyages to deep space. Additionally, for fine attitude determination, star patterns are the most reliable indicator of the attitude of a spacecraft. Stars located far away from the Earth can be treated as fixed points in the inertial frame. They are sufficiently dense on the celestial sphere, making it simple to capture star images at almost any attitude. Star trackers and associated pattern identification techniques have long been investigated. Applications of the various techniques have been successful in several actual space missions.

With unique features such as attitude indicators in space, star trackers are frequently adopted as one of the most accurate attitude sensors. The usual accuracy of these devices is within a few arcseconds, and there is no cumulative error. However, several seconds are required for attitude acquisition when there is no prior attitude information. The main portion of this processing time is used for comparisons between the images obtained by a camera and the ideal images modeled from star catalog in what is termed *star identification*. Consequently, a star identification algorithm can improve the performance of star trackers directly.

There have been many studies related to star identification approach for lost-in-space mode over the past decades [1,2]. They can be categorized roughly into two principal groups: subgraph isomorphism and pattern recognition. The subgraph isomorphism approach compares the angular distance and the length between stars, or the geometric figures. The polygon-based algorithm and match group algorithm can be categorized into this strategy. Among these algorithms, the triangle algorithm is one of the oldest algorithms [3,4]. The brightest stars in the entire image are chosen to form a triangle, and three sides of the triangle and the brightness of each star are compared with those of the database.

The match group algorithm was designed to complement the simple triangle algorithm [5]. The procedure begins with the selection of the brightest stars, and star pairs are generated from these stars. Each star pair is compared with the database, and the stars of database with which the largest number of pairs is matched are identified. This algorithm reduces instances of identification failure, due to the larger number of compared objects relative to those in the triangle algorithm.

Some algorithms that improve the speed of star identification and the robustness to the star position errors have been proposed. Quine and Whyte [6] suggested a binary database search technique to improve the searching speed and Motari et al. [7,8] proposed an even-faster algorithm, the searchless algorithm (SLA). The pyramid algorithm, which uses four stars and their characters for the robustness, was proposed after that [9]. It is also fast, because it employs SLA for improved performance.

Pattern recognition is a strategy that locates the most similar image by comparing the entire image pattern with an onboard database pattern. The grid algorithm [10], the modified-grid algorithm [11], a neural network algorithm [12–14], and a genetic algorithm [15] are classified into this category. The grid algorithm divides the acquired image into grids. If a star exists in a grid cell, the value of the cell is 1; otherwise, it is 0. The entire image becomes a binary pattern in this way and is compared with the database pattern. The structure of grid algorithm is simpler than that of the match group algorithm; moreover, its processing time is shorter [2]. A neural network algorithm and a genetic algorithm are optimized pattern recognition methods, which have training issues or parameter optimization issues. In addition, a singular-value decomposition method was recently proposed by NASA [16]. It is robust to star position uncertainty, but it

Received 2 March 2010; revision received 27 September 2010; accepted for publication 12 October 2010.

*Engineer, Flight Software Team, Space Program Division, Jeonmin-dong, Yuseong; M.S. Candidate, Korea Advanced Institute of Science and Technology, Division of Aerospace Engineering, 335 Gwahangno, Yuseong, 305-701, ROK.

†M.S. Candidate, Division of Aerospace Engineering, 335 Gwahangno, Yuseong.

‡Professor, Division of Aerospace Engineering, 335 Gwahangno, Yuseong. Senior Member AIAA.

cannot be free from star magnitude error and may fail under lack of boresight direction.

In this study, a new star identification method that cross-correlates a camera image with a reference image in the database is proposed. The basic concept originated from pattern recognition. Using a cross-correlation between two star patterns as cost function, the similarity between the acquired star pattern and each of reference star patterns is calculated [17]. A reference pattern that maximizes the cost function can be regarded as the identified pattern. By Fourier transform, the cost function is derived into simple calculation formula. The proposed algorithm provides the possibility of taking advantage of the robustness to star position errors of a pattern recognition strategy.

II. Proposed Algorithm

The new algorithm proposed in this study, created using the correlation approach, finds the most similar star pattern in the star catalog to the star pattern obtained from a camera. Before star identification, the star-pattern image should be reconstructed from the center position of the stars to filter the noise of the original image. The cross-correlation measure between a reference star image from the star catalog and the reconstructed star image from the star camera is then evaluated. By finding the maximum value of the cost function, the most similar star pattern can be identified simultaneously.

A. Arrangement of the Star Image

Before reconstructing the star-pattern image, the star center positions should be arranged by a unified method. Figure 1 shows the entire procedure, which is essentially equivalent to grid algorithm [10].

From the obtained center positions of each star, the star image is modeled. This modeling process must be performed, because the original star image from the camera contains noise. Each star is modeled as a Gaussian distribution, for which the variance depends on the performance of star trackers optics, detector and brightness of the star. The modeled images corresponding to the star positions in Fig. 2 are shown in Fig. 3.

This can be written in terms of a function as follows:

$$A(x,y)=\sum_n \exp\left\{-\frac{(x-x_n)^2+(y-y_n)^2}{2\sigma^2}\right\} \tag{1}$$

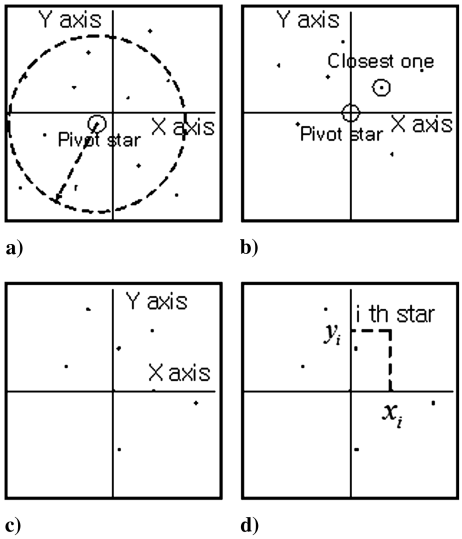

Fig. 1 Arrangement of the star image: a) choose a star of the star image as a pivot star, b) translate the image so that the pivot star is at the center of the image, c) choose the closest star from the pivot star and rotate the image around the pivot star to put the closest star on the positive *X* axis, and d) new positions (x_i, y_i) of stars are obtained.

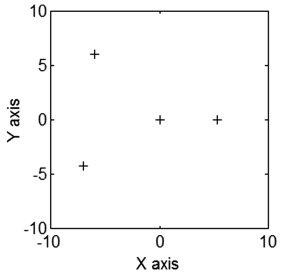

Fig. 2 Center positions of the stars.

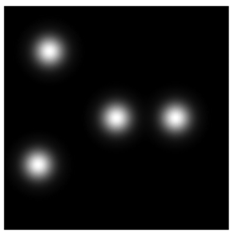

Fig. 3 Modeled star image: top view.

Here, n is the number of stars on the charge-coupled-device (CCD) plane, (x_n, y_n) represents the center position of a star on the CCD plane, and σ^2 denotes the variance of the star image distribution.

B. Cost Function: Correlation

The basic idea of the cost function is the integration of multiplied images. If two images are more similar, the magnitude of the multiplied images will be greater with a large integration output. The corresponding cost function is defined as

$$J=\iint A(x,y)B(x,y)\,\mathrm{d}x\,\mathrm{d}y \tag{2}$$

where

$$A(x,y)=\sum_n \exp\left\{-\frac{(x-x_n)^2+(y-y_n)^2}{2\sigma^2}\right\} \tag{3}$$

is the original image on the CCD plane, and

$$B(x,y)=\sum_m \exp\left\{-\frac{(x-x_m)^2+(y-y_m)^2}{2\sigma^2}\right\} \tag{4}$$

is a similar image in the star catalog. Here, (x_n, y_n) represents the center position of a star on the CCD plane, (x_m, y_m) is the center position of a star in the star catalog, and σ^2 denotes the variance of the star image distribution.

Hence, Eq. (2) is in the form of a cross-correlation of two functions. Therefore, it can be solved using the Fourier transform technique. For a one-dimensional case, the formula can be stated simply as follows:

$$J_0=\int a(x)b(x)\,\mathrm{d}x \tag{5}$$

where

$$a(x)=\sum_n \exp\left\{-\frac{(x-x_n)^2}{2\sigma^2}\right\} \tag{6}$$

$$b(x)=\sum_m \exp\left\{-\frac{(x-x_m)^2}{2\sigma^2}\right\} \tag{7}$$

According to the cross-correlation theorem, the cross-correlation of two functions in Eq. (5) satisfies the following properties, as expressed by Eqs. (8) and (9):

$$h(x) = \int \bar{a}(y)b(x+y)\,\mathrm{d}y \tag{8}$$

$$H(\omega) = \bar{A}(\omega)B(\omega) \tag{9}$$

In these equations, the bar sign denotes the complex conjugate.

As the two functions of Eq. (5) are real functions, the cost function can be written as

$$J_0 = \int_{-\infty}^{\infty} a(x)b(x)\,\mathrm{d}x = \int_{-\infty}^{\infty} \bar{a}(y)b(0+y)\,\mathrm{d}y = h(0) \tag{10}$$

It is known that he Fourier transform and inverse Fourier transform of a Gaussian function is as follows [18]:

$$\Im\{\exp(-\alpha^2 x^2)\} = \frac{1}{\sqrt{2\alpha^2}}\exp\left(-\frac{\omega^2}{4\alpha^2}\right) \tag{11}$$

$$\Im^{-1}\left\{\frac{1}{\sqrt{2\alpha^2}}\exp\left(-\frac{\omega^2}{4\alpha^2}\right)\right\} = \exp(-\alpha^2 x^2) \tag{12}$$

The Fourier transformed function of the one-dimensional images are given by Eq. (13).

$$\begin{aligned} A(\omega) &= \sum_n \exp\{-j\omega x_n\}\sigma\exp\left\{-\frac{\omega^2\sigma^2}{2}\right\} \\ B(\omega) &= \sum_m \exp\{-j\omega x_m\}\sigma\exp\left\{-\frac{\omega^2\sigma^2}{2}\right\} \end{aligned} \tag{13}$$

From Eqs. (8) and (9),

$$H(\omega) = \bar{A}(\omega)B(\omega) = \sum_n\sum_m \exp\{j\omega(x_n - x_m)\}\sigma^2\exp\{-\omega^2\sigma^2\} \tag{14}$$

The term inside the sigma of Eq. (14):

$$\begin{aligned} \exp\{j\omega(x_n - x_m)\}\sigma^2\exp\{-\omega^2\sigma^2\} &= \exp\{j\omega(x_n - x_m)\}\frac{\sigma}{\sqrt{2}} \\ \cdot\frac{1}{\sqrt{2\cdot\frac{1}{4\sigma^2}}}\exp&\left\{-\frac{1}{4\cdot\frac{1}{4\sigma^2}}\omega^2\right\} \end{aligned} \tag{15}$$

Using Eq. (12), the inverse Fourier transform of Eq. (15) is

$$\begin{aligned} &\Im^{-1}\left\{\exp\{j\omega(x_n - x_m)\}\frac{\sigma}{\sqrt{2}}\cdot\frac{1}{\sqrt{2\cdot\frac{1}{4\sigma^2}}}\exp\left\{-\frac{1}{4\cdot\frac{1}{4\sigma^2}}\omega^2\right\}\right\} \\ &= \frac{\sigma}{\sqrt{2}}\exp\left\{-\frac{1}{4\sigma^2}(x - (x_m - x_n))^2\right\} \end{aligned} \tag{16}$$

Thus, the cross-correlation function is derived as follows:

$$h(x) = \sum_n\sum_m \frac{\sigma}{\sqrt{2}}\exp\left\{-\frac{1}{4\sigma^2}(x - (x_m - x_n))^2\right\} \tag{17}$$

Finally, the cost function for one dimension can be expressed as

$$J_0 = h(0) = \sum_n\sum_m \frac{\sigma}{\sqrt{2}}\exp\left\{-\frac{(x_m - x_n)^2}{4\sigma^2}\right\} \tag{18}$$

The two-dimensional cost function is

$$J = \sum_n\sum_m \frac{\sigma^2}{2}\exp\left\{-\frac{(x_n - x_m)^2 + (y_n - y_m)^2}{4\sigma^2}\right\} \tag{19}$$

From Eq. (19), the cross-correlation of two images can be computed with the center coordinates and variance of stars only.

In Eq. (19), the variance of a star, σ^2, is a parameter that needs to be set by users. Technically, it depends on many factors. Some of them are physical phenomena related to star light such as diffraction, aberration or distortion of optics, and photon shot noise. Normally, their effects on the variance tend to vary depending on brightness of stars, spectral class of stars, and positions where star images appear on detectors. It would be more realistic making the new algorithm better if the variance σ^2 is set, in each situation, for each star. However, the constant variance is taken for every star in this study and the following simulations to construct a reference algorithm and show its performance. Assuming a constant-variance position error for all stars, the constant variance in Eq. (19) would exhibit approximate performance to the star position error bound.

C. Database Generation

As shown in Eq. (19), the necessary information is not the entire star image, but every star coordinate in the frame for each pivot star. The coordinates are determined by the arrangement method in Fig. 1. Hence, all star center data for each pivot star constitute the reference database.

D. Star Identification: Correlation Approach

First, the star image from the CCD image plane should be arranged as Fig. 1. Then the cost functions, or cross-correlations, are evaluated from star positions directly as Eq. (19) for every star in the database. The pivot star in the database, which produces the maximum cost function, is the identified star. In short, the star identification algorithm can be expressed in the four steps below.

Step 1) Generate a database from the star catalog using the image arrangement method.

Step 2) Arrange the star image from the CCD plane as Fig. 1 by choosing a pivot star.

Step 3) Evaluate the cost function J using Eq. (19) for all reference patterns.

Step 4) Choose the maximum J and identify the pattern.

To make the star identification faster, the calculation of the exponential function, Eq. (19), can be skipped. If the absolute value inside the exponential function $(x_n - x_m)^2 + (y_n - y_m)^2/4\sigma^2$ is large, then the exponential value will be small enough to be neglected. In this study, the calculation of the term $(x_n - x_m)^2 + (y_n - y_m)^2/4\sigma^2$ being greater than 10 is omitted, because $e^{-10} = 4.54 \times 10^{-5}$ is small enough to ensure that it is not a solution. Moreover, using a limited number of bright stars makes the algorithm faster. For many cases, there are more than 10 stars on the image. In these cases, star identification using only 10 stars results in very similar performance, compared with when all stars are used, while reducing the simulation time and required memory.

The algorithm from step 1 to step 4 identifies one star pattern at a time. Each star of the acquired image could be identified as the closest star on the reference pattern of the star. However, there is always possibility that the pattern was identified erroneously, due to the position error of stars. There is also a possibility that the pivot star or the closest star of the pivot star of the arrangement process (Fig. 1) is a false star. In those cases, the identifications may fail. To increase the identification success rate, several star identification processes from step 1 to step 4 to several pivot stars are recommended. It is reasonable to assume that true stars are more than false stars. With accumulating several identification results of several pivot stars, each star can be identified as having the highest cost or the highest frequency. If we conduct the identification process on every star of the image, the identification rate would be better, whereas the identification time would increase. The tradeoff study between the identification rate and identification time should be regarded.

III. Simulation Study

To verify the performance of the new algorithm, several simulations were conducted. For all simulations, the Skymap 2000 Version 5, published by the NASA Goddard Space Flight Center, was used as a reference star catalog. In the star catalog, 16,916 stars are listed with R-band magnitudes responding to the CCD. After eliminating multiple stars appearing as single stars on the CCD,

14615 stars remained. For convenience, only 4975 stars brighter than a magnitude of 5.5 were used in the simulation. The star camera in this simulation has a 15 deg field of view (FOV), and the resolution is 1024 by 1024 pixels. The simulations were performed by applying position error and false-star error to each star.

The simulation was run for two cases. The first case is for one star identification process from step 1 to step 4 for a pivot star. This case is to evaluate the basic performance of the proposed algorithm and compare the result to the other algorithms. The second case is for star identification with the several processes for several pivot stars. This case is to evaluate the possibility of the algorithm for actual use and the performance of it. In the both cases, the random attitudes that are generated by normal random unit quaternion generator [19,20] of the sensor are assumed for each simulation.

The results of the new algorithm for the first case were compared with those of the grid algorithm [10] and those of the modified-grid algorithm [11] to assess its performance, as grid algorithm is widely used and regarded as an efficient algorithm [2]. Moreover, the strategy of the grid algorithm is somewhat similar to the new algorithm, because it is based on image pattern recognition. The modified-grid algorithm is basically the grid algorithm, but it was modified to increase the identification success rate. In the simulation, the elastic binary grid algorithm of [11] is used, because it only uses the star positions, not the magnitude of them like the proposed algorithm. In the simulations of this study, a 61×61 size grid was used: 16.78×16.78 (1024/61) pixel is a grid.

Only 10 stars were used in the new algorithm when more than 10 stars were readout to reduce the simulation time and required memory. The variance value of the algorithm, σ^2 of Eq. (19), was set as $\sigma = 9 \times \sigma_{\text{error}}$. Because the identification algorithm arranges stars with rotations as Fig. 1, the variance should be different for the positions of stars and increase as the distance from the image center increase. If the variance value is close to the actual, the algorithm would give better results. However, it is hard to predict the exact variance value for every star for every position. The same variance that is large enough to cover outer ones was used for every star on the image, so as to consider actual practices.

A. Star Identification Rate, Case 1: One Identification Process for One Pivot Star

To verify the performance of the algorithm, star centroid position error and false stars were introduced into the image. The position error was applied as Gaussian random noise whose $3\sigma_{\text{error}}$ value ranged from 0 to 5.0 pixels ($\approx$264 arcsec) to the star center position on an image. Although the position error is not realistic, because it actually depends on several things like the brightness of a star or the position on the image, this error could be used to evaluate the basic performance of the identification algorithms to the position error bound. The number of false stars ranged from 0 to 3. The false stars

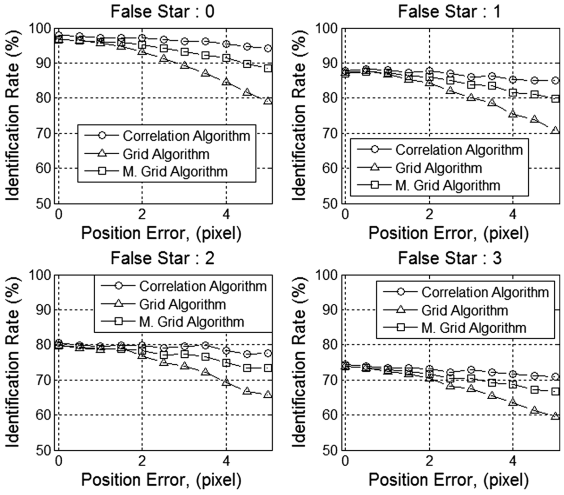

Fig. 4 Identification rate: case 1.

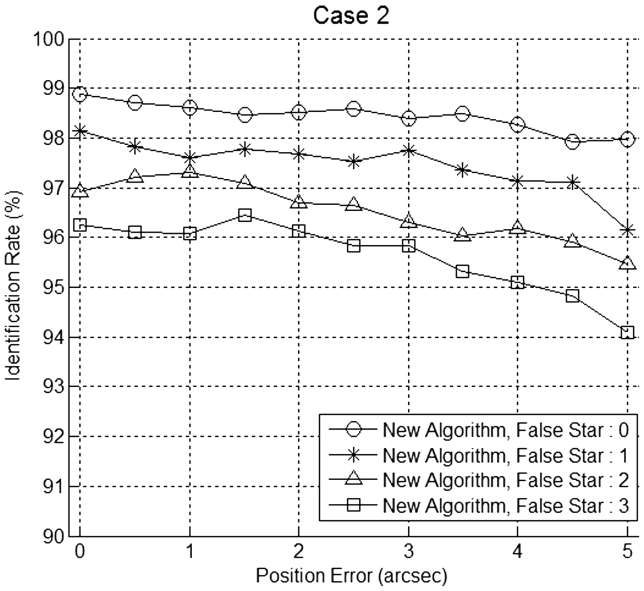

Fig. 5 Identification rate: case 2.

appeared in a random position of the CCD, and the magnitudes were determined by random numbers ranging from 0 to 5. In total, 10,000 identifications were done for each condition. In 70 times out of 10,000 times, 0.7%, the number of stars in the FOV is less than three. The average number of stars in the FOV is 21.24, with the minimum 0 and the maximum 85.

Figure 4 shows plots of the identification rates. As shown in these plots, the identification rates of the new algorithm are superior to those of the grid algorithm and the modified-grid algorithm. For all cases, the new algorithm leads to better identification rates compared with the two other algorithms. In particular, the new algorithm is more robust than the grid algorithm and the modified-grid algorithm for the position error of stars. Against false stars, the three algorithms show similar performance degradation.

B. Star Identification Rate, Case 2: Star Identification for Several Pivot Stars

In case 2, all simulation conditions were identical to those of case 1. Unlike case 1, star identification process was done several times for several pivot stars to overcome the success-rate degradation

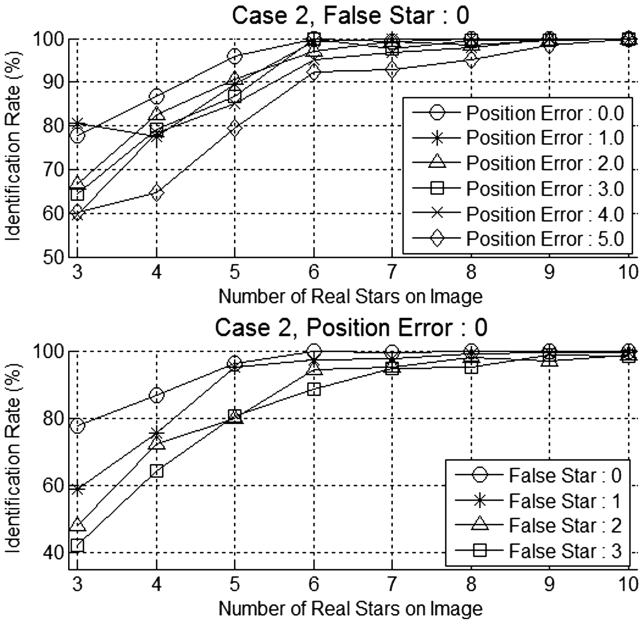

Fig. 6 Identification rates for the number of real stars.

due to position error or false stars. In this simulation, maximum 10 identifications were done for one image. If two or more stars were identified correctly with no wrongly identified star, it was regarded as success in this simulation. Figure 5 shows the identification success rate for the new algorithm. Even though the identification success rate was degraded from 97 to 70% for a single identification process, due to the errors and false stars, the identification rates have improved through several identification processes.

Figure 6 shows the identification rate for the number of real stars in an image. Technically, the minimum number of stars for the identification algorithm is three, because it is impossible to make unique pattern with less than three stars without magnitude information of stars. The upper graph of Fig. 6 is for no false star and the lower one is for zero position error. As the position noise and the number of false stars increase, the identification rate decreases.

C. Star Identification Time

The simulation time for both algorithms was calculated during the simulations. The simulations were conducted on a Microsoft Visual Studio 2008 SP1 C++ x64 platform using an Intel Core 2 Quad Q6600 at 2.4 GHz clock speed. The simulation times for 10,000 times are measured for each algorithm. The results are 34.31 s for the new algorithm, 38.63 s for the grid algorithm and 62.39 s for the modified-grid algorithm. As the results, the new algorithm is faster than the two other algorithms. Although the results are not for actual star trackers, they can be used to briefly illustrate the relative time consumption of the algorithms.

D. Memory Usage

If the data-type float for the position of star and the data-type int for ID is used, the new algorithm, which uses a maximum 10 stars, requires a maximum of 120 N bytes, where N is the number of reference catalog stars. For the grid algorithm and the modified-grid algorithm, there are two different ways to store the pattern data: one is to store the whole grid pattern as one grid at one bit of memory, and the other is to store the grids that contain stars only as a list form. The latter one is efficient for the storage, so the latter form of the grid pattern data was assumed. For the latter storing form, the grid coordinates are stored as int. In this simulation, 577 KB is used for the new algorithm and 1.48 MB is used for the grid algorithm and the modified-grid algorithm. Therefore, the new algorithm is more efficient for memory usage than the two other algorithms.

IV. Conclusions

The algorithm proposed in this study by the correlation approach improves the performance of star-pattern identification. The new algorithm identifies stars by finding the most similar image based on the cross-correlation of a CCD image and a star catalog image, because the cross-correlation is a quantity that represents similarity between two images. The cross-correlation measure of two images is employed as a cost function that should be maximized. Through extensive simulation study, the proposed algorithm turns out to offer several advantages compared with the grid algorithm and the modified-grid algorithm for full sky autonomous star identification, including its robustness in position error, savings in computation time, and more efficient memory use.

References

[1] Spratling, B. B., and Mortari, D., "A Survey on Star Identifications Algorithms," *Algorithms*, Vol. 2, 2009, pp. 93–107.

[2] Nam, M., and Jia, P., "A Survey of All-Sky Autonomous Star Identification Algorithms," *IEEE 1st International Symposium on Systems and Control in Aerospace and Astronautics*, Inst. of Electrical and Electronics Engineers, Piscataway, NJ, 19–21 Jan. 2006, pp. 896–901.

[3] Junkins, J. L., White, C., and Turner, J., "Star Pattern Recognition for Real-Time Attitude Determination," *Journal of the Astronautical Sciences*, Vol. 25, 1977, pp. 251–270.

[4] Groth, E. J., "A Pattern Matching Algorithm for Two-Dimensional Coordinates Lists," *Astronomical Journal*, Vol. 91, 1986, pp. 1244–1248.
doi:10.1086/114099

[5] Bezooijen, R. W. H. V., "True-Sky Demonstration of an Autonomous Star Tracker," *Proceedings of SPIE: The International Society for Optical Engineering*, Vol. 2221, 1994, pp. 156–168.

[6] Quine, B. M., and Whyte, H. F. D. A., "A Fast Autonomous Star-Acquisition Algorithm for Spacecraft," *Control Engineering Practice*, Vol. 4, 1996, pp. 1735–1740.
doi:10.1016/S0967-0661(96)00191-8

[7] Mortari, D., "Search-Less Algorithm for Star Pattern Recognition," *Journal of the Astronautical Sciences*, Vol. 45, No. 2, 1997, pp. 179–194.

[8] Mortari, D., and Neta, B., "K-Vector Range Searching Techniques," 10th Annual AIAA/AAS Space Flight Mechanics Meeting, American Astronautical Society, Paper 00-128 Clearwater, FL, 2000.

[9] Mortari, D., Junkins, J. L., and Samman, M. A., "Lost-in-Space Pyramid Algorithm for Robust Star Pattern Recognition," *Guidance and Control Conference*, Breckenridge, CO, American Astronautical Society, Paper 01-004, 2001.

[10] Padgett, C., and Delgado. K. K., "A Grid Algorithm for Star Identification," *IEEE Transactions on Aerospace and Electronic Systems*, Vol. 33, Jan. 1997, pp. 202–213.

[11] Na, M., Zheng, D., and Jia, P., "Modified Grid Algorithm for Noisy All-Sky Autonomous Star Identification," *IEEE Transactions on Aerospace and Electronic Systems*, Vol. 45, No. 2, April 2009, pp. 516–522.
doi:10.1109/TAES.2009.5089538

[12] Lindsey, C. S., Lindblad, T., and Eide, A. J., "Method for Star Identification Using Neural Networks," *Proceedings of SPIE: The International Society for Optical Engineering*, Vol. 3077, 1997, pp. 471–478.

[13] Kim, K. T., and Bang, H., "Reliable Star Pattern Identification Technique by Using Neural Networks," *Journal of the Astronautical Sciences*, Vol. 52, Nos. 1–2Jan.–June 2004, pp. 239–249.

[14] Hong, J., and Dicjerson, J. A., "Neural-Network-Based Autonomous Star Identification Algorithm," *Journal of Guidance, Control, and Dynamics*, Vol. 23, 2000, pp. 728–735.
doi:10.2514/2.4589

[15] Li, L. H., Zhang, F. E., and Lin, T., "An All-Sky Autonomous Star Map Identification Algorithm Based on Genetic Algorithm," *Opto-Electronic Engineering*, Vol. 27, No. 5, 2000, pp. 15–18.

[16] Juang, J. N., Kim, H. Y., and Junkins, J. L., "An Efficient and Robust Singular Value Method for Star Recognition and Attitude Determination," NASA NASA/TM-2003-212142, 2003.

[17] Kumar, B. V. K. V., Mahalanobis, A., and Juday, R. D., *Correlation Pattern Recognition*, Cambridge Univ. Press, New York, 2005.

[18] Jeffrey, A., and Dai, H., *Handbook of Mathematical Formulas and Integrals*, 4th ed., Academic Press, New York, 2008, p. 357.

[19] Shuster, M. D., "Man, Like These Attitudes are Totally Random!—I. Quaternions," *Advances in the Astronautical Sciences*, Vol. 108, Dec. 2001, pp. 383–396; also 11th AAS/AIAA Space Flight Mechanics Meeting, American Astronautical Society, Paper 01-125, Santa Barbara, CA, Feb. 2001.

[20] Shuster, M. D., "Man, Like These Attitudes are Totally Random!—II. Other Representations," *Advances in the Astronautical Sciences*, Vol. 108, Dec. 2001, pp. 397–408; also 11th AAS/AIAA Space Flight Mechanics Meeting, American Astronautical Society, Paper 01-125, Santa Barbara, CA, Feb. 2001.

D. Spencer
Associate Editor